



## Metataxonomics, metagenomics, metabolomics analysis of the influence of temperature modification in full-scale anaerobic digesters

Francesc Puig-Castellví, Cédric Midoux, Angéline Guenne, Delphine Conteau, Oscar Franchi, Chrystelle Bureau, Céline Madigou, Delphine Jouan-Rimbaud Bouveresse, Pablo Kroff, Laurent Mazéas, et al.

### ► To cite this version:

Francesc Puig-Castellví, Cédric Midoux, Angéline Guenne, Delphine Conteau, Oscar Franchi, et al.. Metataxonomics, metagenomics, metabolomics analysis of the influence of temperature modification in full-scale anaerobic digesters. Bioresource Technology, 2022, 346, pp.126612. 10.1016/j.biortech.2021.126612 . hal-03507080

**HAL Id: hal-03507080**

**<https://hal.inrae.fr/hal-03507080>**

Submitted on 5 Jan 2022

**HAL** is a multi-disciplinary open access archive for the deposit and dissemination of scientific research documents, whether they are published or not. The documents may come from teaching and research institutions in France or abroad, or from public or private research centers.

L'archive ouverte pluridisciplinaire **HAL**, est destinée au dépôt et à la diffusion de documents scientifiques de niveau recherche, publiés ou non, émanant des établissements d'enseignement et de recherche français ou étrangers, des laboratoires publics ou privés.



# Metataxonomics, metagenomics and metabolomics analysis of the influence of temperature modification in full-scale anaerobic digesters

Francesc Puig-Castellví<sup>a,b,1</sup>, Cédric Midoux<sup>b,c,d</sup>, Angéline Guenne<sup>b</sup>, Delphine Conteau<sup>e</sup>, Oscar Franchi<sup>b,f</sup>, Chrystelle Bureau<sup>b</sup>, Céline Madigou<sup>b</sup>, Delphine Jouan-Rimbaud Bouveresse<sup>g</sup>, Pablo Kroff<sup>e</sup>, Laurent Mazéas<sup>b</sup>, Douglas N. Rutledge<sup>a,h</sup>, Gilberte Gaval<sup>e</sup>, Olivier Chapleur<sup>b,\*</sup>

<sup>a</sup> Université Paris-Saclay, INRAE, AgroParisTech, UMR SayFood, 75005 Paris, France

<sup>b</sup> Université Paris-Saclay, INRAE, PRocédés biotechnologiques au Service de l'Environnement, 92160 Antony, France

<sup>c</sup> Université Paris-Saclay, INRAE, MaIAGE, 78350, Jouy-en-Josas, France

<sup>d</sup> Université Paris-Saclay, INRAE, Bioinformatics facility, 78350, Jouy-en-Josas, France

<sup>e</sup> Suez-CIRSEE, 78230 Le Pecq, France

<sup>f</sup> Universidad Adolfo Ibáñez, Facultad de ingeniería y ciencias, 2520000 Viña del mar, Chile

<sup>g</sup> Université Paris-Saclay, AgroParisTech, INRAE, UMR PNCA, 75005 Paris, France

<sup>h</sup> National Wine and Grape Industry Centre, Charles Sturt University, 2650 Wagga Wagga, Australia

## HIGHLIGHTS

- Multi-omics revealed changes in a full-scale anaerobic digester.
- The temperature decrease benefited the growth of the subdominant bacteria.
- At a metagenomics level, Bacteria showed resilience.
- An accumulation of short peptides resulted from the temperature decrease.
- The abovementioned changes led to a lower biogas production.

## ARTICLE INFO

### Keywords:

Metagenomics  
Sub-mesophilic  
Metabolomics  
Full-scale  
Chemometrics

## ABSTRACT

Full-scale anaerobic digesters' performance is regulated by modifying their operational conditions, but little is known about how these modifications affect their microbiome. In this work, we monitored two originally mesophilic (35 °C) full-scale anaerobic digesters during 476 days. One digester was submitted to sub-mesophilic (25 °C) conditions between days 123 and 373. We characterized the effect of temperature modification using a multi-omics (metataxonomics, metagenomics, and metabolomics) approach. The metataxonomics and metagenomics results revealed that the lower temperature allowed a substantial increase of the sub-dominant bacterial population, destabilizing the microbial community equilibrium and reducing the biogas production. After restoring the initial mesophilic temperature, the bacterial community manifested resilience in terms of microbial structure and functional activity. The metabolomic signature of the sub-mesophilic acclimation was characterized by a rise of amino acids and short peptides, suggesting a protein degradation activity not directed towards biogas production.

## 1. Introduction

Anaerobic digestion (AD) is a microbiological process for the

degradation of organic waste that generates biogas (Wang et al., 2019b). The microbial community it involves has a high complexity in terms of diversity and functionality (Vanwonterghem et al., 2014) and is very

\* Corresponding author.

E-mail address: [olivier.chapleur@inrae.fr](mailto:olivier.chapleur@inrae.fr) (O. Chapleur).

<sup>1</sup> Present address: European Genomics Institute for Diabetes, INSERM U1283, CNRS UMR8199, Institut Pasteur de Lille, Lille University Hospital, University of Lille, Lille, France

<https://doi.org/10.1016/j.biortech.2021.126612>

Received 18 October 2021; Received in revised form 17 December 2021; Accepted 18 December 2021

Available online 23 December 2021

0960-8524/© 2022 Elsevier Ltd. All rights reserved.

sensitive to temperature changes (Kim and Lee, 2016). AD can be operated at psychrophilic ( $\leq 20$  °C), mesophilic (30–40 °C) or thermophilic (50–60 °C) conditions (Jain et al., 2015), the last two being the most used at the industrial level. Temperature strongly affects biogas yield, process stability and the potential for process optimization (Westerholm et al., 2018). Anaerobic digestions at higher temperatures are faster and produce higher biogas yields. Besides the elevated biogas production, thermophilic digestion accelerates microbial metabolism in general, including hydrolysis and acidogenesis of recalcitrant feedstock compared to mesophilic conditions (Pasalari et al., 2021). However, mesophilic digestions are more common since they consume less energy (Labatut et al., 2014) and are less susceptible to inhibition by sudden environmental changes (Westerholm et al., 2018).

The temperature effect has been mainly explored in lab-scale digesters (Lin et al., 2016b; Ma et al., 2017; Madigou et al., 2019; Regueiro et al., 2014), while the effect in full-scale digesters has barely been documented (De Vrieze et al., 2015). However, results are not directly extrapolable since volumes in full-scale digesters are larger, kinetics, feeding and mixing are different, and full-scale digesters present a more limited operational control.

At the microbiome level, the temperature effect in AD has mainly been investigated on the basis of temperature changes between mesophilic and thermophilic conditions (Banach et al., 2019; De Vrieze et al., 2015; Ma et al., 2017; Madigou et al., 2019; Westerholm et al., 2017). Conversely, the effect of switching to sub-mesophilic ( $< 30$  °C) conditions has not been much addressed (McKeown et al., 2012; Regueiro et al., 2014). These studies mainly focused on metataxonomics (16S metabarcoding data (Marchesi and Ravel, 2015)), while other biological data were rarely considered (i.e., metagenomics, metatranscriptomics, metabolomics) (Herold et al., 2020; Lin et al., 2017, 2016a). In general, it is assumed that lower temperatures promote acetoclastic methanogenesis (Gunnigle et al., 2013), while hydrogenotrophic archaea such as *Methanobacteriales* grow better in thermophilic environments (Lin et al., 2017). Moreover, the metatranscriptomics results from Lin et al. (2016) suggested that, at higher temperatures, resources are invested towards the central metabolism and the methanogenesis related pathways, enhancing the efficiency of conversion of substrates to methane (Lin et al., 2016a). Since methane conversion is also related to the substrate composition, in practice, the temperature in full-scale digesters is often adjusted depending on the degradability of the loaded waste.

Sub-mesophilic conditions are not rare for full-scale digestion, they can derive from system malfunction but also from the desire to limit heating cost. In this work, we have investigated the effect of switching AD between mesophilic and sub-mesophilic conditions. The temperature of a full-scale digester (reactor B) was decreased from 35 °C to 25 °C, and later switched back to 35 °C. Operated in parallel, a control reactor (reactor A) was maintained under mesophilic conditions. Both systems were characterized with metataxonomics, metagenomics, and metabolomics approaches to unravel the microbiome dynamics following the temperature modification and return to initial conditions. While metagenomics can profile the potential functional interactions between the species involved in AD (Zhang et al., 2019), metabolomics can reveal the outcomes from these interactions. Metabolomics has been recently used to identify the metabolic changes during substrate degradation in AD over time (Herold et al., 2020; Puig-Castellví et al., 2020b). However, from the existing scarce literature it is still unclear if these metabolic changes can also reflect the changes in the digesters' performance. By combining the three omics together, we pursue the characterization of the same AD process at the community (metataxonomics), functional (metagenomics) and molecular (metabolomics) levels. From this work, we expect to gain some insight on how these omics can be used to improve the operational monitoring and management of full-scale anaerobic digesters.

## 2. Materials and methods

### 2.1. Experimental set-up

The full-scale experiment was carried out in France in a wastewater treatment plant (WWTP) with a population equivalent of 190,000. The two 3,000 m<sup>3</sup> full-scale anaerobic digesters (A and B) were operated in parallel and fed with a mixed substrate composed of sewage sludges from wastewater treatment plants and wastes from slaughterhouses. During the time of the experiment, both reactors worked at half capacity due to a constraint in the availability of substrate to treat. The hydraulic retention times (HRTs), organic loading rate (OLRs) and the ambient temperature were monitored but not controlled. On average, the full-scale digesters were operated at a mean hydraulic retention time (HRT) of 34 days and a mean organic loading rate of 0.82 kg of volatile solids m<sup>-3</sup> day<sup>-1</sup>.

The experimental period lasted 462 days. For the first four months of study, the two reactors operated at 35 °C. Reactor A was kept at this temperature during all the experiment. For digester B, the temperature was decreased abruptly to 30 °C on the 123th day and maintained at this level for 2 HRTs until the 190th day. Then, the temperature was modified to 25 °C and maintained for 3 HRTs (between the 191st and the 373th days). Finally, the heating of reactor B was increased from day 374 onwards to reach the initial temperature of 35 °C (Fig. 1A).

### 2.2. Sludge sampling and physico-chemical measurements

Sludge samples from the two reactors were collected at days 0, 80, 177, 218, 281, 353, and 462. Sludge was collected in 50-mL sterile Falcon tubes and immediately transported on dry ice to INRAE, where they were frozen at  $-80$  °C.

Biogas flow, percentage of methane, total ammonia (N-NH<sub>4</sub><sup>+</sup>), chemical oxygen demand (COD), pH, total alkalinity (TAC), total solids (TS), volatile fatty acids (VFA) and volatile matter (VM) were also measured (see supplementary methods).

### 2.3. DNA extraction

For every sample, the total DNA was extracted from 0.2 g of sludge using the DNeasy PowerSoil DNA Elution Kit (Qiagen, Hilden, Germany) following the manufacturer's instruction. DNA was quantified with the Qubit 2.0 Fluorometer (dsDNA BR Assay Kit, Invitrogen, USA).

### 2.4. Metataxonomics

16S DNA sequencing was performed as in Puig-Castellví et al. (2020) (Puig-Castellví et al., 2020a). The V4-V5 regions were amplified using a fusion method (IonAmplicon Library Preparation (FusionMethod) Protocol, Revision C) and sequenced in an Ion Torrent PGM sequencer. Obtained data was processed with FROGS pipeline (Escudié et al., 2018). Details for the bioinformatics analysis of the 16S DNA tags reads are provided in the supplementary methods.

### 2.5. (Meta)genomic DNA sequencing and analysis

The sequencing of the genomic DNA of samples collected on days 80, 177, 218, 281 and 462 was carried out.

Libraries were prepared with the TruSeq NGS Library Prep Kit from Westburg (WB9024) and sequencing was done using the Illumina NextSeq 500, generating 150 bp paired end reads (NextSeq 500 High Output Kit 300 cycles).

Bioinformatics analysis was performed to refine, assemble, annotate and count the sequences. Data from bacteria and archaea were further processed separately. The count matrices were arranged into blocks by grouping KEGG ORTHOLOGY (KO) identifiers from the same KEGG PATHWAY (Kanehisa et al., 2017) in the same block. Finally, the blocks

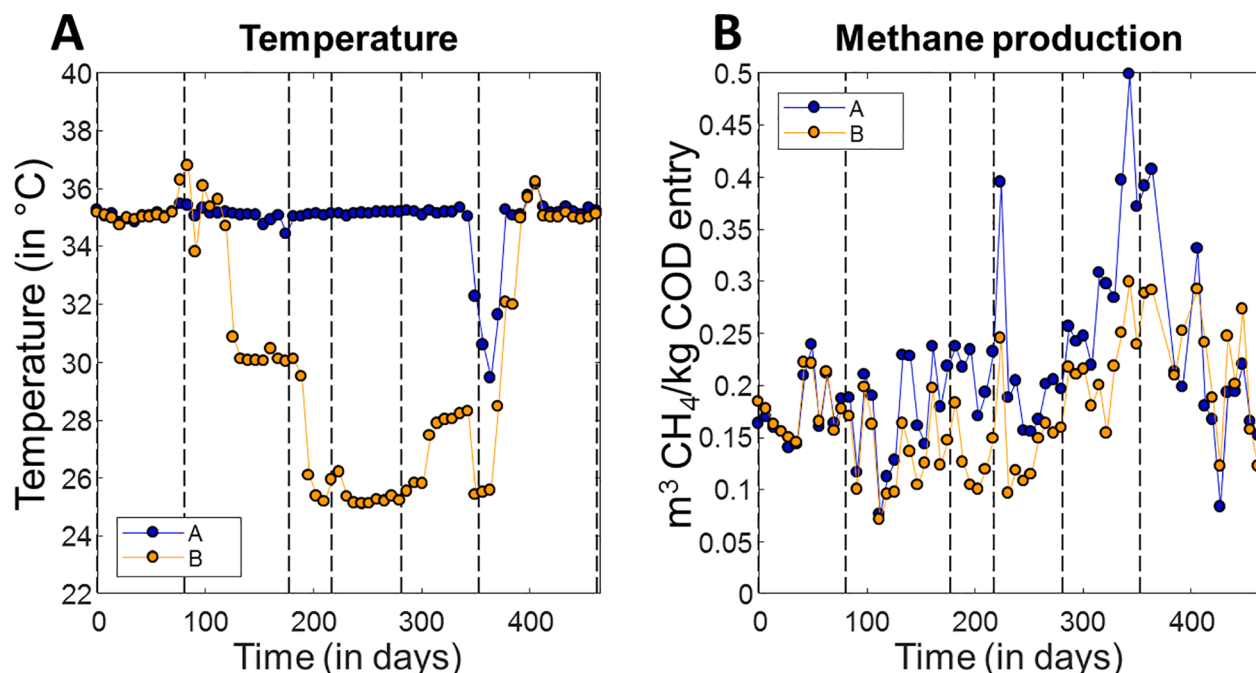


Fig. 1. A) Reactor temperatures. B) Methane production, expressed in cubic meters per kg of COD in reactor inlets. Digester A is represented in blue while reactor B is colored in orange. The sampling dates are indicated by the dashed lines.

were auto-scaled and analyzed with ComDim.

ComDim is an exploratory chemometric method that calculates a series of orthogonal common dimensions (or CDs) as linear combinations of the original variables. For every CD, the global scores (representative of the consensus for all the blocks), the local scores (representative of the samples within each block) the loadings (representative of the variables), and the weights (representative of the blocks' importance) are calculated. For more information regarding ComDim, see (El Ghaziri et al., 2016; Qannari et al., 2001). CD loadings were converted to hexadecimal color values and these values were used to color the KEGG PATHWAYS maps. See the supplementary methods for the detailed protocol.

## 2.6. Metabolomics analysis

Four aliquots with 0.75 mL of sludge were extracted per reactor and time-point. The extracts were analyzed with a HPLC-MS system equipped a NUCLEODUR HILIC column (Macherey-Nagel, Düren, Germany) and a LTQ-Orbitrap XL mass spectrometer (Thermo Scientific, Waltham, MA, USA) operated in positive electrospray ionization mode (ESI<sup>+</sup>). Chromatographic features were extracted from the HPLC-MS spectra using XCMS Online platform (Tautenhahn et al., 2012). Significant features were selected using a non-targeted strategy and tentatively assigned after employing collision-induced dissociation (CID) fragmentation and consulting the Metlin platform (Guijas et al., 2018). See the supplementary methods for the detailed protocol.

## 2.7. Network analysis

The network analysis is based on the calculation of the Pearson's correlation among the relative abundances of the detected archaeal genus and bacterial orders, the metagenomics profiles obtained from the two ComDim analyses and the PC scores of the metabolomics data. Only the values from the common time-points screened across the 3 omics platforms (days 80, 177, 218, 281 and 462) were used for this analysis. The network graph was built using the *igraph* R-package (Csardi and Nepusz, 2006). Only correlations above 0.8 or below -0.8 are displayed.

## 3. Results and discussion

### 3.1. The temperature decrease caused a lower methane production

The methane production (Fig. 1B) of both reactors was similar ( $99 \pm 8\%$ <sub>B/A</sub>) until the temperature was modified in reactor B at the 123th day (Fig. 1A), at which point its methane production became 76% of that of reactor A. This tendency was observed during all the time the two reactors were maintained at different temperatures ( $70 \pm 10\%$ <sub>B/A</sub>).

The temperature switch also produced a pH acidification, a lower alkalinity, an increase of VS, TS, and COD levels, and a reduction of the total ammonia levels. VFA levels were comparable between the two digesters (Supplementary material), denoting that the decrease in methane production was not derived from methanogenic inhibition due to the presence of these molecules.

After returning to 35 °C, the methane production of both reactors became similar again and the differences in pH and alkalinity were reduced.

### 3.2. Subdominant bacteria rose during the sub-mesophilic conditions

Overall, the microbial diversity consisted of 2,773 OTUs (48 archaeal and 2,725 bacterial OTUs).

From the 48 archaeal OTUs, 7 were found in a relative abundance higher than 0.1% in at least one of the samples (Fig. 2A). Of these 7 (dominant) archaeal OTUs, 5 were assigned to *Euryarchaeota* and another to a *Crenarchaeota* (OTU<sub>59</sub>). The *Euryarchaeota* phylum comprises most methanogens. From this phylum, 3 OTUs were assigned to *Methanobrevibacter*, *Methanolinea*, and *Methanosaeta* genera. Both *Euryarchaeota* (Ciotola et al., 2013; Lin et al., 2017; Regueiro et al., 2014) and *Crenarchaeota* (Cai et al., 2016; Ciotola et al., 2013) have been previously found in AD systems.

The archaeal profile in reactor A was more stable over time than that in reactor B. In both reactors, at 35 °C, the relative abundances of the archaea were between ~ 2.7% and ~ 4.2%. In reactor A, a transient temperature decrease near the 353th day caused a momentary reduction of the archaeal population down to ~ 2.2%. In reactor B, the applied temperature decrease also caused a reduction of the archaeal population

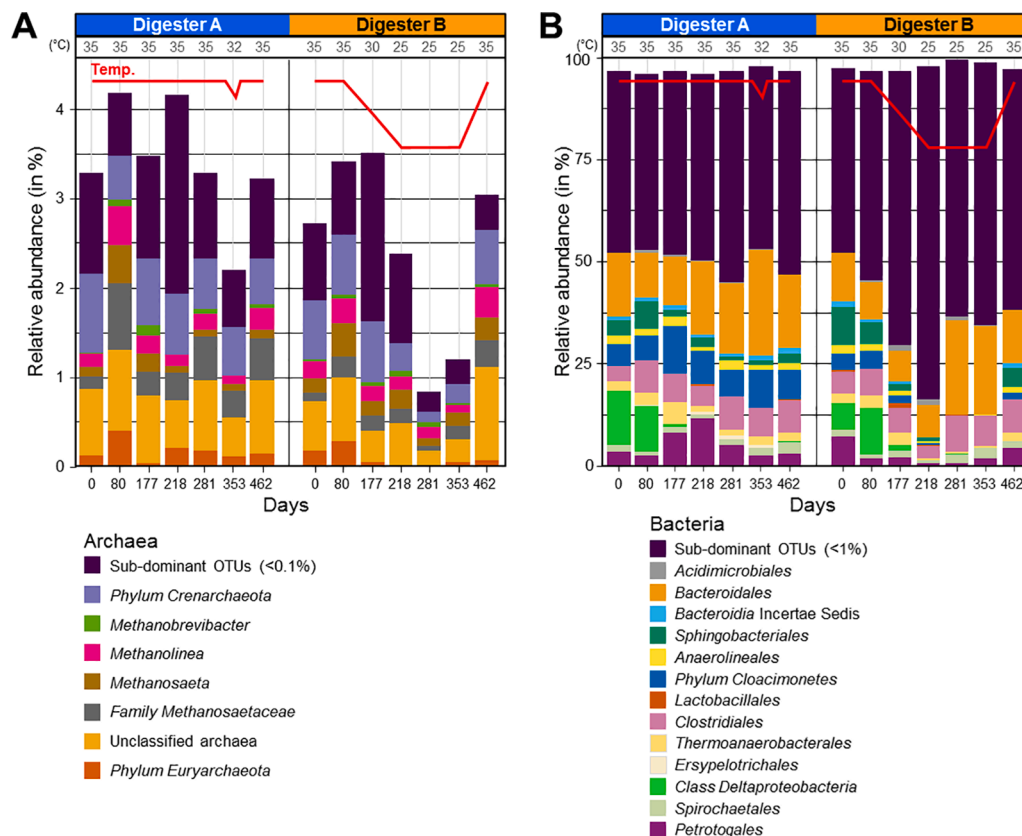


**Fig. 2.** Microbial structure in the reactors. **A)** Archaeal structure. **B)** Bacterial structure. Archaeal OTUs were grouped by genus, and bacterial OTUs were grouped by order. Sub-dominant groups include all the OTUs found in a relative abundance inferior to the cut-off level (0.1% for the archaea and 1% for the bacteria) in all the samples. Reactor temperature is given at the top of the bars with values and graphically illustrated with a red line.

that reached its lowest relative abundance ( $\sim 0.28\%$ ) at the 281st day. This effect on the archaeal community may explain the reduction of the methane production (Fig. 1). Methanogenesis is considered a rate-limiting step due to its sensitivity to environmental changes (Wang et al., 2019a). Moreover, this decrease was not the same for all OTUs, as the *Euryarchaeota* unassigned at the phylum level and the *Crenarchaeota* were more affected than the others.

We compared the microbial structure in the undisturbed reactor and in the disturbed reactor, after return to mesophilic conditions. The archaeal community show little resilience, as observed by a larger contribution of the unclassified archaea (yellow bars in Fig. 1A) and a smaller contribution of the sub-dominant archaea (dark purple in Fig. 1A) at the end of the experiment in reactor B compared to reactor A. Regueiro et al. (2014) found that *Methanosaeta* was one of the few methanogenic archaea able to recover (Regueiro et al., 2014). A similar observation for this microorganism can be drawn from our data.

The reduced resilient character of Archaea can also be noted from the PCA analysis in Fig. 3A. In this figure, the temporal evolution of the archaeal profile cannot be easily drawn, suggesting that the observed differences between samples at the same temperature are due to other underlying factors besides the time progression.

The bacteria accounted for  $\sim 95.8\%$  and  $\sim 99.2\%$  of the relative abundance in the reactors. Of the 2,725 OTUs, 56 OTUs were found in a relative abundance higher than 1% in at least one of the samples while the rest were considered to be sub-dominant on basis to this threshold.

The more prominent bacterial taxa are the orders *Bacteroidia* Incertae Sedis, *Petrotogales*, *Clostridiales* and *Bacteroidales*; and the phylum *Cloacimonetes*. This profile was similar to previous microbiome characterizations of full-scale biogas plants (Calusinska et al., 2018; Westerholm et al., 2018).

In both reactors, the *Deltaproteobacteria* and the *Sphingobacteriales*

reduced dramatically their relative abundance after the 80th day allegedly as the result of a change common to both reactors systems (i.e. feeding modification).

As expected, the temperature modification in reactor B altered its bacterial structure. The microbial community consisting of the sub-dominant OTUs increased its relative abundance when the temperature was decreased to  $30^\circ\text{C}$  ( $\sim 66\%$  of the relative abundance), and its proportion was even higher after reducing the temperature to  $25^\circ\text{C}$  ( $\sim 81\%$ ). This response suggests that the most prevalent microorganisms in the reactors cannot rapidly acclimate, allowing the contribution of the sub-dominant microorganisms to expand. In fact, 21 sub-dominant OTUs showed a strong negative correlation ( $r < -0.9$ ) with the temperature. Of these 21, the 3 most abundant were OTU\_394 (*Clostridia* *Christensenellaceae*), OTU\_445 (*Bacteroidia* Incertae Sedis *Draconibacteriaceae*), and OTU\_492 (*Sphingobacteriales* *Chitinophagaceae*). *Bacteroidales* are acidogenic, sugar-fermenting, saccharolytic and proteolytic bacteria that produce propionate, acetate and succinate (Cardinali-Rezende et al., 2012). *Christensenella* ferment simple sugars (Morotomi et al., 2011) and can establish syntrophic relationships with methanogenic archaea through  $\text{H}_2$ -transfer (Ruaud et al., 2020). This important change in the overall microbial structure derived from the bacterial population may have caused ecological instabilities that led to the aforementioned decrease of the archaeal population by the 281st day. To sum up, the broad effect on the microbial (archaeal and bacterial) community indicates that all the steps of the AD (hydrolysis, acidogenesis, acetogenesis and methanogenesis) were affected by the temperature modification.

After temperature was set again at  $35^\circ\text{C}$ , some of the dominant microorganisms were able to recover their position in the reactor. This was the case for the mesophilic bacteria *Cloacimonetes*, which went from  $\sim 4.2\%$  at  $35^\circ\text{C}$  to  $< 0.1\%$  at  $25^\circ\text{C}$ , but returned to  $\sim 1.6\%$  at  $35^\circ\text{C}$  at



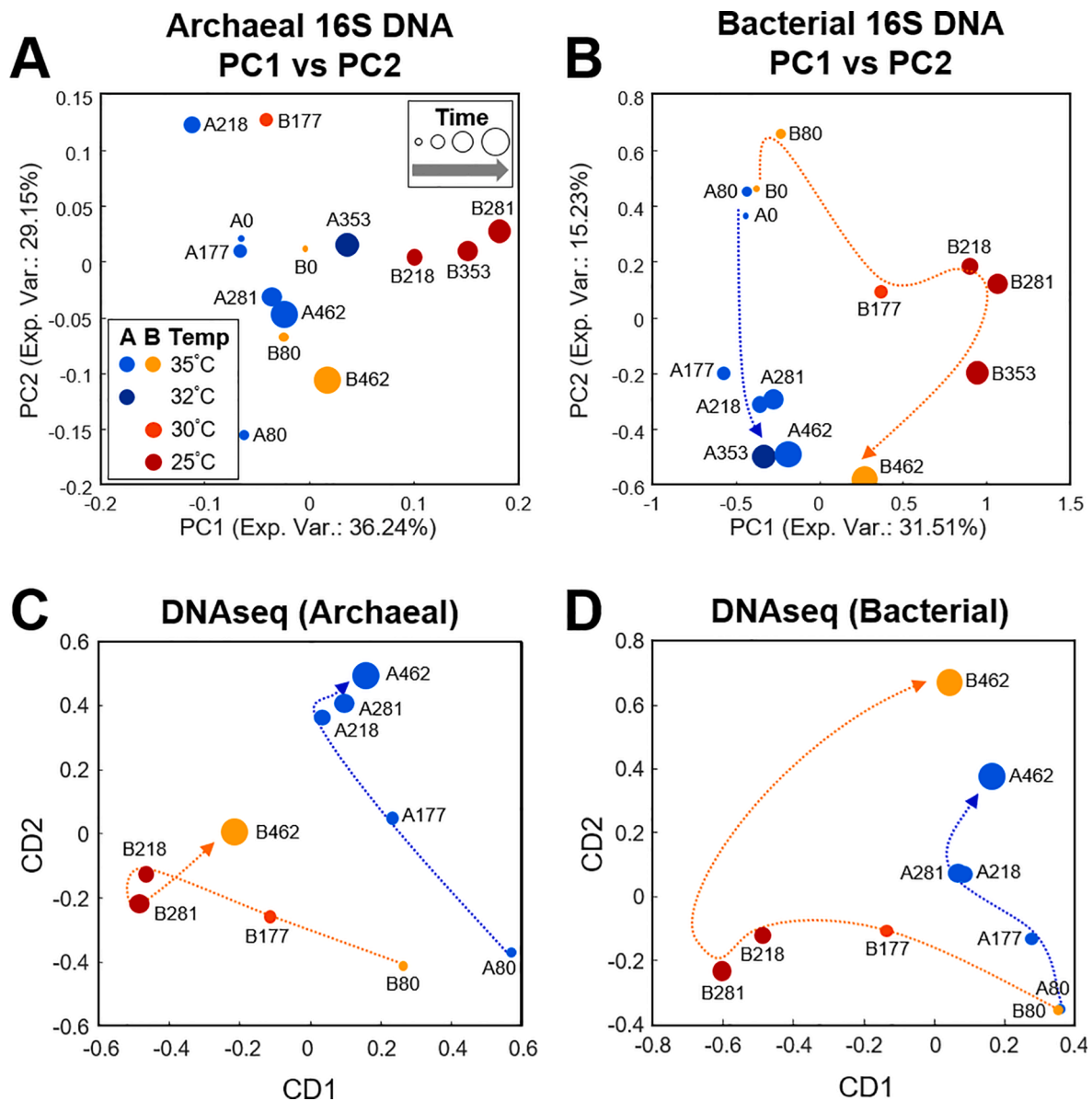


**Fig. 3.** (A–B) PCA analyses of the archaeal (A) and bacterial (B) structure in the reactors, obtained from the 16S metataxonomics data. (C–D) Global scores obtained in the ComDim analyses of the archaeal (C) and the bacterial (D) data sets based on DNaseq metagenomics data. In the figure, samples are labelled with the letter of the digester “A” for the control digester, “B” for the temperature-changing digester) and the day. The temporal evolution of the two reactors is represented by blue and orange dashed lines for digesters “A” and “B” respectively.

the end of the study. In the PCA of Fig. 3B, it can be noted that the evolution of the two reactors converge at the 462th day. The resilient capabilities of the bacterial communities from anaerobic digesters after being exposed to temperature alterations have been documented before (Luo et al., 2015; Westerholm et al., 2017). In addition, and in line with our results, Luo et al. (2015) only observed resilience for the bacterial community but not for the archaeal one. The divergences in the adaptability performance of the archaeal and bacterial communities might be explained by the lower species redundancy in the archaea, a lower growth rate and by the fact that the natural habitat of some (if not most) archaea are extreme environments (Mayer and Müller, 2014) and therefore are more sensitive and less prepared to grow under mesophilic and sub-mesophilic conditions than are the bacteria.

### 3.3. Archaeal potential functional activity was less resilient than the bacterial one to the temperature modification

The millions of gene sequence reads in the metagenomics analyses represent molecular functions from a few hundreds of pathways. In order to preserve this data structure in the multivariate data analysis, the metagenomics data was analyzed with ComDim, which is a chemometric method intended for the analysis of multi-blocks datasets (see Materials and methods). Specifically, in this analysis, each dataset block represented one KEGG PATHWAY (Kanehisa et al., 2017). Two ComDim analyses were performed to investigate the metagenomics data from the archaeal (Fig. 4A) and the bacterial (Fig. 4B) communities. These two communities were well described by the first two components, CD1 and CD2, in each analysis. In the two analyses, the global scores in CD1 were descriptive of the metagenomics differences due to the temperature (negative scores were associated with samples from lower temperatures, and vice versa for the positive scores), while the global scores in CD2

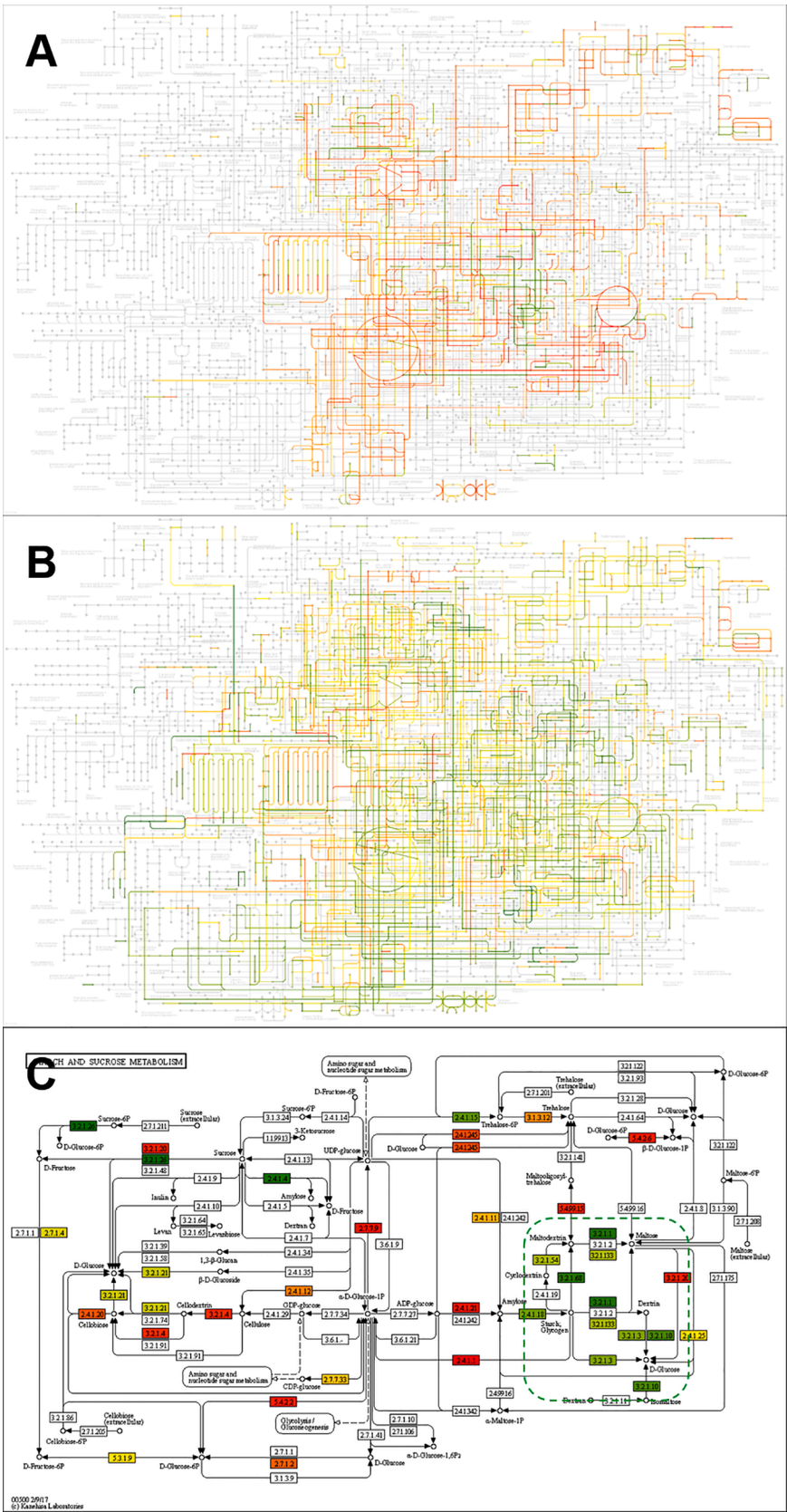


**Fig. 4.** KEGG maps of the main metabolic pathways colored according to CD1 from the (A) archaeal and the (B) bacterial metagenomics datasets. (C) Metabolic pathway for starch and sucrose metabolism, colored according to CD1 in Archaea. Genes in red are associated with positive loadings (more abundant in samples at 35 °C), genes in green with negative values (more abundant in samples at 25 °C), genes in yellow to loadings with 0 values (no change), and a gradient of these colors was used for intermediate loading values. The green dashed box in (C) denotes a cluster of genes more abundant at 25 °C. The biological maps for CD2 loadings are given in the supplementary material.

were linked to the evolution of the reactors over time (positive scores associated to the time progression).

Lowering the temperature in reactor B generated a divergence of its metagenomics profile from that of reactor A at both the archaeal and the bacterial level (Fig. 4). Restoring the mesophilic temperature in the reactor B did not have the same effect in both communities. While it drove the bacterial metagenomics profiles of the two reactors closer, the archaeal metagenomics profile of reactor B remained distant from that of reactor A after the perturbation is ended. This difference denotes a higher resilience capability for the bacterial community than for the archaeal community, as the metataxonomics data showed.

### 3.4. Archaeal potential functional activity switched to starch metabolism

The analysis of the molecular functions encoded by the metagenomics data was done from 2 complementary perspectives. First, the local ComDim scores were examined to investigate the metagenomics profiles at the biological pathway level, as each set of local scores corresponds to one biological pathway. The plots for the local ComDim scores from 135 pathways (45 for archaea, 90 for bacteria) are given in the [Supplementary material 1](#). In a second approach, the loadings values from the ComDim analysis presented in the previous section, which are representative of each of the genes within each pathway, were plotted in KEGG maps to evaluate their importance. These maps are given in the [Supplementary material 2-5](#).

On the one hand, the local scores showed that the temperature modulates all the biological pathways. Bacterial and archaeal adaptations to temperature include modifications of the lipid cell membranes (Siliakus et al., 2017), but also the accumulation of osmolytes, changes in DNA and protein conformation, alteration of translation and cell signaling mechanisms, among others (Cavicchioli, 2006; Shivaji and Prakash, 2010). Hence, the process of temperature adaptation resulted on the alteration of most of the cellular events. Interestingly, while the local scores distribution for nearly all the bacterial blocks resulted in similar profiles, highlighting the already mentioned resilience of the bacterial community, the evolution of the local scores of the archaeal blocks was more heterogeneous.

On the other hand, the inspection of the ComDim loadings in the KEGG maps revealed different metabolic effects of temperature in archaea and bacteria.

In archaea, most of the genes were more abundant at 35 °C (red genes in Fig. 4A and [Supplementary material 2](#)). This behavior was most prevalent for the “glycolysis (ko00010)”, “tricarboxylic citric acid cycle (ko00020)”, “pentose phosphate pathway (ko00030)”, “purine metabolism (ko00230)”, “pyrimidine metabolism (ko00240)”, and most of the amino acids biosynthetic pathways. Other pathways mildly affected were “methane metabolism (ko00680)”, and “oxidative phosphorylation (ko00190)”. Conversely, the genes presenting a higher count number at lower temperatures (green genes in [Supplementary material 2](#)) were associated with the L-cysteine biosynthesis from L-serine (in “glycine, serine, and threonine metabolism” (ko00260)), the transformation of starch to glucose (in “starch and sucrose metabolism” (ko00500), Fig. 4C), and the L-arginine conversion to L-ornithine (in “arginine biosynthesis” (ko00220)). Moreover, genes related to the biosynthesis of all aminoacyl-tRNAs (ko00970) except for L-pyrrolysyl-tRNA were diminished due to the temperature decrease. L-pyrrolysine is an amino acid required to translate proteins for initiating methanogenesis from methylamines (Gaston et al., 2011). In general, it can be interpreted that the decrease of the temperature caused a decline in the gene counts for the main biochemical processes, whereas starch became an important source of carbon under these conditions.

The effect of time (described by CD2), in overall, shows a higher abundance of all the genes at the earlier time-points (green genes in [Supplementary material 3](#)). From those, some notably affected pathways include “glycolysis (ko00010)”, “biosynthesis of porphyrin and chlorophyll (ko00860)”, and the genes involved in “ribosome biogenesis”

(ko03009). This could be interpreted as the metabolic activity at the beginning of the experiment was higher because the feeding may be richer in nutrients. Nevertheless, some genes were more predominant at the later time-points (red genes in [Supplementary material 3](#)), such as those required for trehalose and amylose biosynthesis (in “starch and sucrose metabolism” (ko00500)), the genes for assimilating pyruvate into the tricarboxylic citric acid cycle (in “glycolysis” (ko00010)), and those from the same cycle (ko00020) leading to oxoglutarate. Thus, the metabolic activity at the later time-points is mainly characterized by anabolic reactions (including the synthesis of saccharides and some amino acids that use oxoglutarate as a carbon skeleton).

In bacteria, the response was more heterogeneous than in archaea. This can be understood as the functional diversity of the bacteria is in principle much more complex.

In bacteria, the metabolic activity was higher at 25 °C rather than at 35 °C, as denoted by the abundance of the genes colored in green in Fig. 4B. More details of this figure can be seen in [Supplementary material 4](#). In part, this is in agreement with the major presence of the bacterial community as shown from the metataxonomics data (Fig. 2). Still, some effects were detected in the synthesis of spermidine (in “glutathione metabolism” (ko00480)), the pathway related to “one carbon pool” (ko00670), and the “ribosome biogenesis” (ko03009). The latter suggests that the temperature decrease caused a silencing of protein translation. Regarding the synthesis of spermidine, polyamines are known to be necessary to grow at high temperatures (Michael, 2018). Alternatively, more genes from some specific pathways found to be accumulated at lower temperatures (green genes in [Supplementary material 4](#)), such as those from the Entner-Doudoroff pathway (in the “pentose phosphate pathway” (ko00030)), the “ascorbate and aldarate metabolism” (ko00053), the “nitrogen metabolism” (ko00910), the “sulfur metabolism” (ko00920), the metabolic pathways from some amino acids, the “glutathione metabolism” (ko00480), the “ubiquinone and other terpenoid-quinone biosynthesis” (ko00130), the “benzoate degradation” (ko00362) and the “aminobenzoate degradation” (ko00627). In all, this denotes that the bacterial community was in general more favored at 25 °C.

Finally, CD2 revealed that the pathways related to “lipopolysaccharide biosynthesis” (ko00540) and to “riboflavin biosynthesis” (ko00740) had important contributions at the early stages of the experiment (green genes in [Supplementary material 5](#)). At the later stages, the number of genes presenting prominent contributions (red genes in [Supplementary material 5](#)) was not very high and these genes were not located at specific pathways as in the previous cases. This broad distribution could indicate that the metabolic activity at the later time-points is lower in general than that at the earlier time-points.

### 3.5. Temperature decrease influenced degradation pathways

The sludge samples were investigated with untargeted HPLC-MS metabolomics, detecting a total of 700 features representative of sludge. These data were explored by PCA (Fig. 5) in order to identify the major sources of variance that drive the metabolomics differences across samples. The first 3 PCs captured 38.06% of the dataset variance. The first component (PC1, 15.97% of the explained variance) mainly showed the sample distribution across time, and the second component (PC2, 13.43%) separated the samples according to the reactors' temperature.

More in detail, the PCA showed no differences between reactors at the beginning of the study, and they started to diverge after the modification of the temperature in reactor B at the 123th day.

The three samples from digestions carried out at  $\leq 30$  °C were identified by negative scores in PC1 and by positive scores in PC2 (Fig. 5A). Moreover, these samples did not cluster together, indicating that the metabolic activity in the reactor was not stable for this period. However, since the samples from day 353 in reactor B clustered with those from reactor A, despite their temperature difference, common stability may have been achieved by that time. Having said this, after



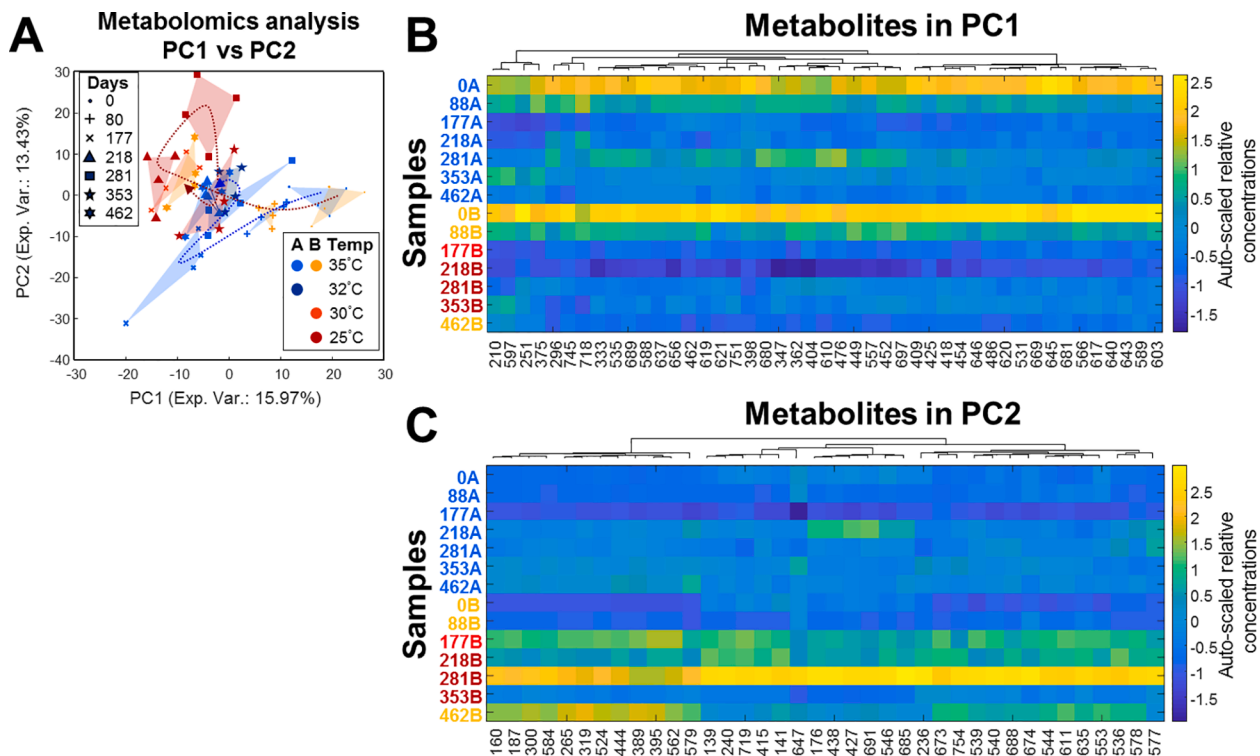


**Fig. 5.** A. PCA analysis of the LC-MS metabolomics peak areas dataset. B-C). Heatmap of the selected features in PC1 (B) and PC2 (C). In the PCA, replicate samples were grouped together and the evolution of the digester was drawn with dashed arrows, as in Fig. 3. In the heatmaps, samples are colored ranging from dark blue (less concentrated) to yellow (more concentrated). Metabolic features are represented by numbers in the x-axis of the heatmaps. More detail on these features can be consulted in supplementary material.

changing the temperature back to 35 °C, the reactor's stability was affected again and the metabolomic activity continued evolving towards more negative scores in PC1.

The features selected in PC1 (Fig. 5B) showed the same trend over time for the two digesters, which suggest they are indicative of the same modification in both digesters (e.g. substrate feeding). This pattern describes a notorious decrease until day 218, followed by a small rise peaking around day 281, and a plateau for the final part of the study. The observed decrease in these features may be connected to the decay of the *Deltaproteobacteria* and the *Sphingobacteriales* observed in the metataxonomics analysis.

The metabolites selected in PC1 showed an extremely high chemical complexity, as the molecular masses for the selected features were between 750 and 1,200 uma. Due to that, we are unable to propose clear tentative identifications for most of these features even after screening the exact masses on comprehensive databases such as Massbank (Horai et al., 2010) and Metlin (Guijas et al., 2018). Nevertheless, on the basis of their H/C and O/C ratios (see supplementary material), they could correspond to unsaturated hydrocarbons.

The features selected in PC2 showed a prominent peak at 25 °C (Fig. 5C). These were mainly assigned to amino acids, di-peptides, tri-peptides, and nucleosides (see supplementary material), reflecting a protein degradation profile that agrees with the more acidic pH observed when reactor B operated under sub-mesophilic conditions (supplementary material). PC2 metabolic response may be also connected to the TS, VS, and COD parameters, as they were more elevated in B after the temperature modification (supplementary material).

The high contribution of these metabolites in PC2 may be the consequence of the lower efficiency of the community in the digester to consume amino acids and peptides during acidogenesis. The lower amino acid uptake could also explain the lower translation activity observed in bacteria from the metagenomics analysis. Moreover, the accumulation of protein catabolism metabolites may also explain why

the metabolic pathways linked to amino acid metabolism are some of the few that showed resilience in archaea.

### 3.6. The observed changes in the three omics data are correlated

In order to see how the different omics relate to each other, a network analysis was made.

The metagenomics data had strong correlations to other variables. The CD1 archaeal metagenomics profile (CD1\_arc in Fig. 6) correlated with the CD1 bacterial metagenomics profile (CD1\_bac in Fig. 6), as both describe the microbial adaptation to temperature. These two CD1s are anti-correlated with the relative abundance of the sub-dominant bacteria. As commented, the decrease of the temperature resulted in a major contribution of this polyphyletic group, possibly due to the faster adaptation of these sub-dominant bacteria to the new environmental conditions. The negative correlation of the sub-dominant bacteria with *Cloacimonetes* indicated that the latter was not able to acclimate while the sub-dominant was. Moreover, CD1\_arc is positively correlated with OTU\_121 (*Euryarchaeota*), while CD1\_bac is correlated with *Anaerolineales* and *Bacteroidia* Incertae Sedis (Ana and BacIn in Fig. 6, respectively). In both cases, the temperature decrease caused a notable reduction in the species' contribution to the microbial structure.

At a metabolomics level, PC1 positively correlated with OTU\_121 as they were both affected in reactor B during the temperature decrease. On the other hand, PC2 inversely correlated with the *Anaerolineales*, the *Cloacimonetes* (Cloac in Fig. 6) and the *Thermoanaerobacterales* (Therm in Fig. 6).

Finally, within the metataxonomics data, two clusters of strong correlations were found. First, the *Sphingobacteriales*, the *Methanolinea* and the *Methanosaeta* showed positive correlations among them all. Second, the *Deltaproteobacteria* showed positive correlations with the *Sphingobacteriales* and the *Methanosaeta*, but also with the *Euryarchaeota*. The *Deltaproteobacteria* and the *Sphingobacteriales* are degraders, and the

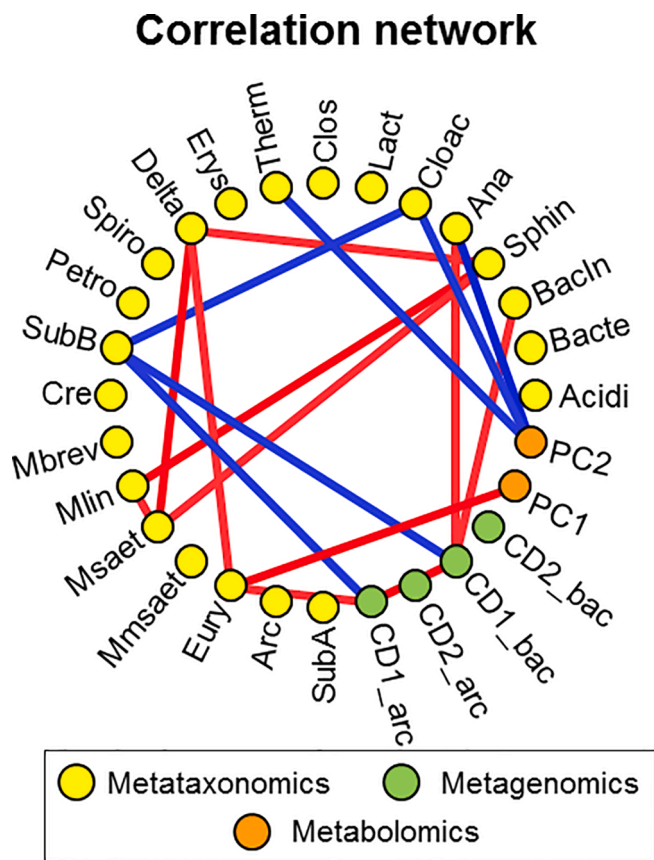


**Fig. 6.** Correlation network. Only correlations above 0.8 (in red) and below  $-0.8$  (in blue) are shown. Node labels of 16S rDNA data: Acidi, *Acidimicrobiales*; Bacte, *Bacteroidales*; BacIn, *Bacteroidia* Incertae Sedis; Sphin, *Sphingobacteriales*; Ana, *Anaerolineales*; Cloac, *Cloacimonetes*; Lact, *Lactobacillales*; Clos, *Clostridiales*; Therm, *Thermoanaerobacterales*; Erys, *Erysipelotrichales*; Delta, *Deltaproteobacteria*; Spiro, *Spirochaetales*; Petro, *Petrotogales*; SubB, Subdominant Bacteria; Cre, *Crenarchaeota*; Mbrev, *Methanobrevibacter*; Mlin, *Methanolinea*; Msaet, *Methanosaeta*; Mmsaet, *Methanosaetaceae*; Eury, *Euryarchaeota*; Arc, Archaea; SubA, Subdominant Archaea.

molecules resulting from their metabolism may be used by the archaeal community, leading to the establishment of syntrophic relationship among them.

### 3.7. Combining different omics provides a larger biological picture of the AD microbiome

Omics analyses, as standalone studies, can only provide one layer of information that is sometimes difficult to interpret by itself. However, in multi-omics analyses, the different layers give complementary intertwined information that results in a better global picture. In this study, the 3 tested omics approaches were proven suitable to study AD, as the changes in the metagenomics data could be easily related to changes in the microbial structure and resulted on detectable metabolic variations. Despite that, these three omics methods cannot be regarded as equivalent as they present intrinsic differences in terms of omics coverage.

By modifying the reactor operational set-up from mesophilic to sub-mesophilic conditions, a partial replacement of the bacterial core by subdominant species occurred, which eventually also led to the repression of the archaeal growth, causing a reduction of the methane production. Thus, the observed discrepancies in the previous literature may also be derived from a different latent sub-dominant microbial community.

At a functional level, at 25 °C the bacterial community was more active, except for some specific pathways such as those involved in protein translation. Conversely, the metabolic activity in archaea

inferred from the metagenomics data was globally reduced. Archaea are more sensitive than bacteria (Madigou et al., 2019), and therefore may be more altered due to this temperature modification. The higher sensitivity in archaea was also indicated by their lower resilience capabilities towards temperature.

The observed enhancement of the overall metabolic activity in bacteria may be a consequence of the sub-dominant bacteria more favored to grow at sub-mesophilic than at mesophilic conditions. Consistent with the latter, at a metabolic level, the temperature modification caused an accumulation of nitrogen-containing metabolically assimilable compounds including amino acids and peptides, among others. These metabolic and physicochemical changes in the reactors fostered microbial community alterations that resulted in a less efficient (rate-limiting) acidogenesis, observed by the reduced levels of total ammonia (Fig S6) since the nitrogen-containing metabolites were not being degraded. Because of or in addition to this metabolic impairment, the methanogenic archaea's growth was inhibited ultimately leading to the lower biogas production (Fig. 1B).

Besides, as protein degradation slowed down, utilization of other nutrients may have increased. In this line, the rise of the sub-dominant *Clostridia Christensenellaceae* and *Bacteroidia* Incertae Sedis *Draconibacteriaceae* suggests a shift to the utilization of starch and sugar. This would explain why the reduction of the archaeal population (observed in the metataxonomics data) was delayed on time, as it occurred as a response to the limited acidogenesis resulting from the modification of the bacterial structure. Moreover, the shift towards starch metabolism may also have existed for the archaea since the metagenomics data showed an increase of the corresponding gene counts.

On an operational view, even if sub-mesophilic AD produce less biogas, a lesser amount of this biogas is needed to heat the reactor. Then, the process could be still considered as economically viable. Accounting that sub-mesophilic AD may be less prone to process failures than mesophilic AD since the levels of total ammonia (a process inhibitor) were lower (supplementary material), it can be regarded as a promising waste management strategy.

## 4. Conclusions

The temperature decrease in the digester was marked by a partial replacement of the bacterial core microbiome and a reduction of the contribution of the archaea to the total microbial community. Regarding the latter, the archaeal population was distorted to the extent that it was unable to recover the original state once the temperature was restored at the end of the experiment.

Moreover, the alteration of the microbial community led to a modification of the overall metabolic activity, resulting on an accumulation of short peptides by the 281st day as well as a lower biogas production.

## Uncited references

### CRediT authorship contribution statement

**Francesc Puig-Castellví:** Methodology, Software, Formal analysis, Data curation, Writing – original draft, Visualization. **Cédric Midoux:** Formal analysis. **Angéline Guenne:** Investigation. **Delphine Conteau:** Conceptualization, Resources, Supervision. **Oscar Franchi:** Investigation. **Chrystelle Bureau:** Investigation. **Céline Madigou:** Investigation. **Delphine Jouan-Rimbaud Bouveresse:** Supervision, Writing – review & editing. **Pablo Kroff:** Resources, Supervision, Funding acquisition. **Laurent Mazéas:** Methodology, Writing – review & editing, Supervision, Project administration, Funding acquisition. **Douglas N. Rutledge:** Methodology, Software, Writing – review & editing, Supervision, Funding acquisition. **Gilberte Gaval:** Conceptualization, Writing – review & editing, Supervision. **Olivier Chapleur:** Conceptualization, Methodology, Writing – review & editing, Supervision, Funding

acquisition.

## Declaration of Competing Interest

The authors declare that they have no known competing financial interests or personal relationships that could have appeared to influence the work reported in this paper.

## Acknowledgements

The authors acknowledge the plant operators from SUEZ group hosting the full-scale trial and providing the sludge samples, the high-throughput sequencing facility of I2BC for its sequencing and bioinformatics expertise, and the INRAE MIGALE bioinformatics facility (MIGALE, INRAE, 2020. Migale bioinformatics Facility, doi: 10.15454/1.5572390655343293E12) for the provided computing resources.

## Funding

This work is part of the DIGESTOMIC project funded by the National Research 470 Agency (ANR-16-CE05-0014)

## Appendix A. Supplementary data

Supplementary data to this article can be found online at <https://doi.org/10.1016/j.biortech.2021.126612>.

## References

- Banach, A., Ciesielski, S., Bacza, T., Pieczykowski, M., Ziemińska-Buczyńska, A., 2019. Microbial community composition and methanogens' biodiversity during a temperature shift in a methane fermentation chamber. *Environ. Technol. (United Kingdom)* 40 (24), 3252–3263. <https://doi.org/10.1080/09593330.2018.1468490>.
- Cai, M., Wilkins, D., Chen, J., Ng, S.-K., Lu, H., Jia, Y., Lee, P.K.H., 2016. Metagenomic Reconstruction of Key Anaerobic Digestion Pathways in Municipal Sludge and Industrial Wastewater Biogas-Producing Systems. *Front. Microbiol.* 7, 778. <https://doi.org/10.3389/fmicb.2016.00778>.
- Calusinska, M., Goux, X., Fossépré, M., Muller, E.E.L., Wilmes, P., Delfosse, P., 2018. A year of monitoring 20 mesophilic full-scale bioreactors reveals the existence of stable but different core microbiomes in bio-waste and wastewater anaerobic digestion systems. *Biotechnol. Biofuels* 11, 196. <https://doi.org/10.1186/s13068-018-1195-8>.
- Cardinali-Rezende, J., Colturato, L.F.D.B., Colturato, T.D.B., Chartone-Souza, E., Nascimento, A.M.A., Sanz, J.L., 2012. Prokaryotic diversity and dynamics in a full-scale municipal solid waste anaerobic reactor from start-up to steady-state conditions. *Bioreour. Technol.* 119, 373–383. <https://doi.org/10.1016/j.biortech.2012.05.136>.
- Cavicholi, R., 2006. Cold-adapted archaea. *Nat. Rev. Microbiol.* 4 (5), 331–343. <https://doi.org/10.1038/nrmicro1390>.
- Ciotola, R., Martin, J., Castaño, J., Lee, J., Michel, F., 2013. Microbial Community Response to Seasonal Temperature Variation in a Small-Scale Anaerobic Digester. *Energies* 6, 5182–5199. <https://doi.org/10.3390/en6105182>.
- Csardi, G., Nepusz, T., 2006. The igraph Software Package for Complex Network Research. *InterJournal. Complex Systems*.
- De Vrieze, J., Saunders, A.M., He, Y., Fang, J., Nielsen, P.H., Verstraete, W., Boon, N., 2015. Ammonia and temperature determine potential clustering in the anaerobic digestion microbiome. *Water Res.* 75, 312–323. <https://doi.org/10.1016/j.watres.2015.02.025>.
- El Ghaziri, A., Cariou, V., Rutledge, D.N., Qannari, E.M., 2016. Analysis of multiblock datasets using ComDim: Overview and extension to the analysis of (K + 1) datasets. *J. Chemom.* 30 (8), 420–429. <https://doi.org/10.1002/cem.2810>.
- Escudé, F., Auer, L., Bernard, M., Mariadassou, M., Cauquil, L., Vidal, K., Maman, S., Hernandez-Raquet, G., Combes, S., Pascal, G., 2018. FROGS: Find, Rapidly, OTUs with Galaxy Solution. *Bioinformatics* 34 (8), 1287–1294.
- Gaston, M.A., Zhang, L., Green-Church, K.B., Krzycki, J.A., 2011. The complete biosynthesis of the genetically encoded amino acid pyrrolysine from lysine. *Nature* 471 (7340), 647–650. <https://doi.org/10.1038/nature09918>.
- Guijas, C., Montenegro-Burke, J.R., Domingo-Almenara, X., Palermo, A., Warth, B., Hermann, G., Koellensperger, G., Huan, T., Uritboonthai, W., Aisporna, A.E., Wolan, D.W., Spilker, M.E., Benton, H.P., Siuzdak, G., 2018. METLIN: A Technology Platform for Identifying Knowns and Unknowns. *Anal. Chem.* 90 (5), 3156–3164. <https://doi.org/10.1021/acs.analchem.7b04424>.
- Gunnigle, E., McCay, P., Fuszard, M., Botting, C.H., Abram, F., O'Flaherty, V., 2013. A functional approach to uncover the low-temperature adaptation strategies of the archaeon *Methanosarcina barkeri*. *Appl. Environ. Microbiol.* 79 (14), 4210–4219. <https://doi.org/10.1128/AEM.03787-12>.
- Herold, M., Martínez Arbas, S., Narayanasamy, S., Sheik, A.R., Kleine-Borgmann, L.A.K., Lebrun, L.A., Kunath, B.J., Roume, H., Bessarab, I., Williams, R.B.H., Gillece, J.D., Schupp, J.M., Keim, P.S., Jäger, C., Hoopmann, M.R., Moritz, R.L., Ye, Y., Li, S., Tang, H., Heintz-Buschart, A., May, P., Müller, E.E.L., Laczny, C.C., Wilmes, P., 2020. Integration of time-series meta-omics data reveals how microbial ecosystems respond to disturbance. *Nat. Commun.* 11, 5281. <https://doi.org/10.1038/s41467-020-19006-2>.
- Horai, H., Arita, M., Kanaya, S., Nihei, Y., Ikeda, T., Suwa, K., Ojima, Y., Tanaka, K., Tanaka, S., Aoshima, K., Oda, Y., Kakazu, Y., Kusano, M., Tohge, T., Matsuda, F., Sawada, Y., Hirai, M.Y., Nakanishi, H., Ikeda, K., Akimoto, N., Maoka, T., Takahashi, H., Ara, T., Sakurai, N., Suzuki, H., Shibata, D., Neumann, S., Iida, T., Tanaka, K., Funatsu, K., Matsuura, F., Soga, T., Taguchi, R., Saito, K., Nishioka, T., 2010. MassBank: A public repository for sharing mass spectral data for life sciences. *J. Mass Spectrom.* 45 (7), 703–714. <https://doi.org/10.1002/jms.1777>.
- Jain, S., Jain, S., Wolf, I.T., Lee, J., Tong, Y.W., 2015. A comprehensive review on operating parameters and different pretreatment methodologies for anaerobic digestion of municipal solid waste. *Renewable and Sustainable Energy Reviews* 52, 142–154. <https://doi.org/10.1016/j.rser.2015.07.091>.
- Kanehisa, M., Furumichi, M., Tanabe, M., Sato, Y., Morishima, K., 2017. KEGG: new perspectives on genomes, pathways, diseases and drugs. *Nucleic Acids Res.* 45 (D1), D353–D361. <https://doi.org/10.1093/nar/gkw1092>.
- Kim, J., Lee, C., 2016. Response of a continuous anaerobic digester to temperature transitions: A critical range for restructuring the microbial community structure and function. *Water Res.* 89, 241–251. <https://doi.org/10.1016/j.watres.2015.11.060>.
- Labatut, R.A., Angenent, L.T., Scott, N.R., 2014. Conventional mesophilic vs. thermophilic anaerobic digestion: A trade-off between performance and stability? *Water Res.* 53, 249–258. <https://doi.org/10.1016/j.watres.2014.01.035>.
- Lin, Q., De Vrieze, J., He, G., Li, X., Li, J., 2016a. Temperature regulates methane production through the function centralization of microbial community in anaerobic digestion. *Bioreour. Technol.* 216, 150–158. <https://doi.org/10.1016/j.biortech.2016.05.046>.
- Lin, Q., De Vrieze, J., Li, C., Li, J., Li, J., Yao, M., Hedenec, P., Li, H., Li, T., Rui, J., Frouz, J., Li, X., 2017. Temperature regulates deterministic processes and the succession of microbial interactions in anaerobic digestion process. *Water Res.* 123, 134–143. <https://doi.org/10.1016/j.watres.2017.06.051>.
- Lin, Q., De Vrieze, J., Li, J., Li, X., 2016b. Temperature affects microbial abundance, activity and interactions in anaerobic digestion. *Bioreour. Technol.* 209, 228–236. <https://doi.org/10.1016/j.biortech.2016.02.132>.
- Luo, G., De Francisci, D., Kougias, P.G., Laura, T., Zhu, X., Angelidaki, I., 2015. New steady-state microbial community compositions and process performances in biogas reactors induced by temperature disturbances. *Biotechnol. Biofuels* 8, 3. <https://doi.org/10.1186/s13068-014-0182-y>.
- Ma, K.-L., Li, X.-K., Wang, K.-e., Ren, Y.-H., Chu, Z.-R., Zhang, J., 2017. Role of temperature on microbial community profiles in an anaerobic bioreactor for treating PTA wastewater. *Chem. Eng. J.* 308, 256–263. <https://doi.org/10.1016/j.cej.2016.09.064>.
- Madigou, C., Lê Cao, K.-A., Bureau, C., Mazéas, L., Déjean, S., Chapleur, O., 2019. Ecological consequences of abrupt temperature changes in anaerobic digesters. *Chem. Eng. J.* 361, 266–277. <https://doi.org/10.1016/j.CEJ.2018.12.003>.
- Marchesi, J.R., Ravel, J., 2015. The vocabulary of microbiome research: a proposal. *Microbiome* 3, 31. <https://doi.org/10.1186/s40168-015-0094-5>.
- Mayer, F., Müller, V., 2014. Adaptations of anaerobic archaea to life under extreme energy limitation. *FEMS Microbiol. Rev.* 38 (3), 449–472. <https://doi.org/10.1111/1574-6976.12043>.
- McKeown, R.M., Hughes, D., Collins, G., Mahony, T., O'Flaherty, V., 2012. Low-temperature anaerobic digestion for wastewater treatment. *Curr. Opin. Biotechnol.* 23 (3), 444–451. <https://doi.org/10.1016/j.copbio.2011.11.025>.
- Michael, A.J., 2018. Polyamine function in archaea and bacteria. *J. Biol. Chem.* 293 (48), 18693–18701. <https://doi.org/10.1074/jbc.TM118.005670>.
- Morotomi, M., Nagai, F., Watanabe, Y., 2011. Description of *Christensenella minuta* gen. nov., sp. nov., isolated from human faeces, which forms a distinct branch in the order Clostridiales, and proposal of Christensenellaceae fam. nov. *Int. J. Syst. Evol. Microbiol.* 62, 144–149. <https://doi.org/10.1099/ijs.0.026989-0>.
- Pasalari, H., Gholami, M., Rezaee, A., Esrafil, A., Farzadkia, M., 2021. Perspectives on microbial community in anaerobic digestion with emphasis on environmental parameters: A systematic review. *Chemosphere* 270, 128618. <https://doi.org/10.1016/j.chemosphere.2020.128618>.
- Puig-Castellví, F., Cardona, L., Bureau, C., Bouveresse, D.-R., Cordella, C.B.Y., Mazéas, L., Rutledge, D.N., Chapleur, O., 2020a. Effect of ammonia exposure and acclimation on the performance and the microbiome of anaerobic digestion. *Bioreour. Technol. Reports* 11, 100488. <https://doi.org/10.1016/j.biteb.2020.100488>.
- Puig-Castellví, F., Cardona, L., Jouan-Rimbaud Bouveresse, D., Cordella, C.B.Y., Mazéas, L., Rutledge, D.N., Chapleur, O., 2020b. Assessment of substrate biodegradability improvement in anaerobic Co-digestion using a chemometrics-based metabolomic approach. *Chemosphere* 254, 126812. <https://doi.org/10.1016/j.chemosphere.2020.126812>.
- Qannari, E.M., Courcoux, P., Vigneau, E., 2001. Common components and specific weights analysis performed on preference data. *Food Qual. Prefer.* 12 (5-7), 365–368. [https://doi.org/10.1016/S0950-3293\(01\)00026-X](https://doi.org/10.1016/S0950-3293(01)00026-X).
- Regueiro, L., Carballa, M., Lema, J.M., 2014. Outlining microbial community dynamics during temperature drop and subsequent recovery period in anaerobic co-digestion systems. *J. Biotechnol.* 192, 179–186. <https://doi.org/10.1016/j.jbiotec.2014.10.007>.
- Ruad, A., Esquivel-Elizondo, S., de la Cuesta-Zuluaga, J., Waters, J.L., Angenent, L.T., Youngblut, N.D., Ley, R.E., Blaser, M.J., 2020. Syntrophy via interspecies H<sub>2</sub> transfer between *Christensenella* and *Methanobrevibacter* underlies their global

- cooccurrence in the human gut. *MBio* 11 (1). <https://doi.org/10.1128/mBio.03235-19>.
- Shivaji, S., Prakash, J.S.S., 2010. How do bacteria sense and respond to low temperature? *Arch. Microbiol.* 192 (2), 85–95. <https://doi.org/10.1007/s00203-009-0539-y>.
- Siliakus, M.F., van der Oost, J., Kengen, S.W.M., 2017. Adaptations of archaeal and bacterial membranes to variations in temperature, pH and pressure. *Extremophiles* 21 (4), 651–670. <https://doi.org/10.1007/s00792-017-0939-x>.
- Tautenhahn, R., Patti, G.J., Rinehart, D., Siuzdak, G., 2012. XCMS online: A web-based platform to process untargeted metabolomic data. *Anal. Chem.* 84 (11), 5035–5039. <https://doi.org/10.1021/ac300698c>.
- Vanwonterghem, I., Jensen, P.D., Ho, D.P., Batstone, D.J., Tyson, G.W., 2014. Linking microbial community structure, interactions and function in anaerobic digesters using new molecular techniques. *Curr. Opin. Biotechnol.* 27, 55–64. <https://doi.org/10.1016/j.copbio.2013.11.004>.
- Wang, M., Zhou, J., Yuan, Y.-X., Dai, Y.-M., Li, D., Li, Z.-D., Liu, X.-F., Zhang, X.-Y., Yan, Z.-Y., 2019a. Methane production characteristics and microbial community dynamics of mono-digestion and co-digestion using corn stalk and pig manure. *Int. J. Hydrog. Energy*. 42 (8), 4893–4901. <https://doi.org/10.1016/j.ijhydene.2016.10.144>.
- Wang, N.-X., Lu, X.-Y., Tsang, Y.-F., Mao, Y., Tsang, C.-W., Yueng, V.A., 2019b. A comprehensive review of anaerobic digestion of organic solid wastes in relation to microbial community and enhancement process. *J. Sci. Food Agric.* 99 (2), 507–516. <https://doi.org/10.1002/jsfa.9315>.
- Westerholm, M., Isaksson, S., Karlsson Lindsjö, O., Schnürer, A., 2018. Microbial community adaptability to altered temperature conditions determines the potential for process optimisation in biogas production. *Appl. Energy* 226, 838–848. <https://doi.org/10.1016/j.apenergy.2018.06.045>.
- Westerholm, M., Isaksson, S., Sun, L.i., Schnürer, A., 2017. Microbial Community Ability to Adapt to Altered Temperature Conditions Influences Operating Stability in Anaerobic Digestion. *Energy Procedia* 105, 895–900.
- Zhang, L.e., Loh, K.-C., Lim, J.W., Zhang, J., 2019. Bioinformatics analysis of metagenomics data of biogas-producing microbial communities in anaerobic digesters: A review. *Renewable and Sustainable Energy Reviews* 100, 110–126. <https://doi.org/10.1016/j.rser.2018.10.021>.